CHAPTER- VIII

DAMPING CHARACTERISTICS OF HOMOGENEOUS AND STRATIFIED SOIL-ASH DEPOSIT

8.1 INTRODUCTION

The damping ratio exhibits a greater degree of change than the dynamic shear modulus, particularly under high strain. Therefore, it is important to ascertain the damping behavior of soil that has been subjected to a load that produces high strain. The damping ratio is commonly estimated using a symmetric hysteresis loop formed between shear stress and shear strain plot. In the cyclic triaxial test, the symmetric hysteresis loop gets converted into an asymmetric hysteresis loop, especially under large shearing strain observed in various studies (Jaya et al., 2012; Kokusho, 1980; Kumar et al., 2017). A "spindle-shaped" hysteresis loop was observed at small-strain, whereas an "S-shaped" hysteresis loop was observed under a large strain, according to Nogami et al. (2012). Kumar et al. (2017) incorporated the asymmetric hysteresis loop for the damping evaluation and found a unique profile of the damping versus shear strain, which increases with shear strain and attains a maximum at 1% shear strain and then decreases continuously. On the other hand, most of the past studies considered only symmetric loop and shows the continuously increasing profile of the damping versus shear strain. Chakrabortty et al. (2020) and Das and Chakraborty (2022) considered asymmetric hysteresis loop and modified the ASTM method along with the conventional method to

determine the variation in damping ratio. From the results, it was concluded that symmetric methods underestimate the damping value, whereas asymmetric method gives a higher damping value. Mog and Anbazhagan (2022) also implemented two approaches (Steady state vibration-SSV and Free vibration decay-FVD) in the Resonant column test. It is advised to use the SSV approach for small strains, whereas the FVD method may work better for medium strains.

From the above-mentioned literature, this can be concluded that most of the research is focused on the liquefaction study of stratified sandy materials. Apart from that, past studies are associated with a limited number of variables (e.g., single loading frequency) which can be seen in Table 8.1. In addition, these samples are subjected to very narrow shear strain during cyclic loading. Furthermore, the dynamic characteristics, particularly the damping behavior of stratified soil deposit is different from that of the homogeneous soil deposit, and very limited studies have been carried out considering the stratification of waste materials and their damping properties. Therefore, it is significant to investigate the damping characteristics of the stratified soil (soil-ash) deposit for the safe design of geotechnical structures resting on it. Also, the specimen preparation techniques used in the past studies were cumbersome and time-consuming, which can be eliminated by employing the simple technique used in the present study.

The research gap discussed above from the literature gives the motivation for the present investigation, which has been fulfilled by performing experimental determination of the damping characteristics of homogeneous and stratified soil-ash deposits using cyclic triaxial tests. The influence of relative compaction, loading frequency, and confining pressure on the damping ratio with varying shear strain has been implemented for a better understanding of the composite system. In addition, the

influence of the shape of the hysteresis loop on the damping characteristics has been evaluated by using three different methods such as Symmetric Hysteresis Loop (SHL), Asymmetric Hysteresis Loop (ASHL), and the modified American Society for Testing and Materials (ASTM) method. The precise estimation of the damping ratio helps in the close prediction of ground responses under seismic excitations.

8.2 SIGNIFICANCE OF DAMPING PROPERTIES

The significance of the present study must be emphasized so that it can be better correlated with the field which will increase its widespread acceptability during the application. As a result, this section explains the necessity of the present study in the current context. The quantity of coal ash produced every year creates a huge amount of accumulation near the ash disposal location. These disposal locations are not properly designed to sustain such huge loads that give rise to the failure of such dams due to the deposition of consecutive layers every year. In order to minimize the disastrous effect of coal ash on the environment, a new practical application area/material must be proposed. The present study specifically concentrated on the application of fly ash as pavement subgrade or embankment fill material. The pavement construction involves a considerable amount of capital; therefore, a complete study is required under static and dynamic loading conditions before the application of fly ash in the field. Hence, an attempt has been made here to determine the damping properties of homogeneous and layered soil-ash deposits. Because the damping properties of the material have a substantial impact on the behavior of the deposit under seismic conditions.

8.3 METHODOLOGY AND EXPERIMENTAL PROGRAM

The shear modulus and damping ratio are the two fundamental dynamic soil properties of soil that can be calculated from the hysteresis loop generated during the cyclic

loading. The shear modulus is the slope of the line drawn from the origin to max/min peaks of the hysteresis loop plotted between shear stress versus shear strain. However, the damping ratio is evaluated after calculating the area of the hysteresis loop that represents the dissipation of energy and the area of the shaded portion that represents the potential energy stored, as shown in Fig. 8.1. In general, the soil behavior is nonlinear elastoplastic when cyclic shear strain (γ) crosses the strain range of 0.1% (> 0.1%) (Ishihara, 1996). The shape of the hysteresis loop highly depends upon the shear strain level, which means the shape of the hysteresis loop changes from symmetric to asymmetric as the shear strain increases from small to large. Based on the different shapes and calculation approaches, the methods are divided into three forms such as 1) SHL, 2) ASHL, and 3) ASTM, which can be seen in Fig. 8.1 (Das and Chakrabortty, 2022). From Fig. 8.1 and Table 8.1, this can be observed that the determination of shear modulus requires only the secant Young's modulus both in the extension and compression side. The secant Young's modulus is independent of the shape of the hysteresis loop rather it depends on the max/min peak of the loop. As per the definition, the damping ratio is dependent on the shape of the hysteresis loop and the asymmetricity at large strain influences the shape of the loop because of the variation in the peaks of the stress-strain relationship (Kokusho, 1980; Kumar et al., 2017). Kokusho (1980) first incorporated the effect of asymmetricity in damping ratio calculation which was further modified by Kumar et al. (2017) and named as the ASHL approach. According to the ASTM D-3999 (1996), the SHL approach was considered as a standard method, but several researchers have observed a remarkable difference in the damping ratio estimated from the ASHL method as compared to the SHL approach (Das and Chakrabortty, 2022; Jaya et al., 2012; Kumar et al., 2017). The asymmetricity plays a significant role in the accurate estimation of the damping ratio. Hence, especially in the

case of large shear strain, the damping ratio must be checked with all the methods, so that the error involved can be identified.

Table 8.1. Expressions that estimate the dynamic characteristics using various methodologies.

Approach	Damping ratio	Secant Young's modulus (E_{sec})	Secant shear modulus (G_{sec})	Shear strain (γ)
Symmetric hysteresis loop	$D_{initial} = \frac{1}{4\pi} * \frac{A_L}{A_\Delta}$	$E_{sec,\,initial} = (E_{sec1} + E_{sec1})/2$	$G_{sec,\,initial} = \frac{(E_{sec,initial})}{2(1+\upsilon)}$	$\gamma = (1+\upsilon) * \varepsilon$
Asymmetric hysteresis loop	$D_{initial} = \frac{1}{\pi} * \frac{A_{L(o-a-b-c-d)}}{A_{\Delta 1}+A_{\Delta 2}+A_{\Delta 3}}$			
Modified ASTM	$D_{initial} = \frac{1}{\pi} * \frac{A_L}{\left(\frac{1}{2}*\sigma_{d,max}*\varepsilon_{max} + \frac{1}{2}*\sigma_{d,min}*\varepsilon_{min}\right)/2}$			

A total of 105 strain-controlled cyclic triaxial tests were performed in the present study. A detailed schematic experimental plan/testing program has been shown in Fig. 8.2. The input variables like relative compaction, frequency of loading, confining pressure, and cyclic shear strain have been considered for the study. Both the homogeneous and stratified soil-ash samples (diameter 50mm and height 100 mm) were prepared under relative compaction (RC) of 95%, 97%, and 99%. The tests were conducted under the cyclic shear strain (γ) of 0.3 to 1.5% considering loading frequencies of 0.3, 0.5, & 1 Hz. The confining pressures of 70, 80, and 100 kPa have been taken into consideration to examine the impact of the overburden pressure. The stratified sample was prepared in two-layered forms, i.e., fly ash at the top and local soil at the bottom. The tests were conducted under consolidated undrained (CU) conditions.

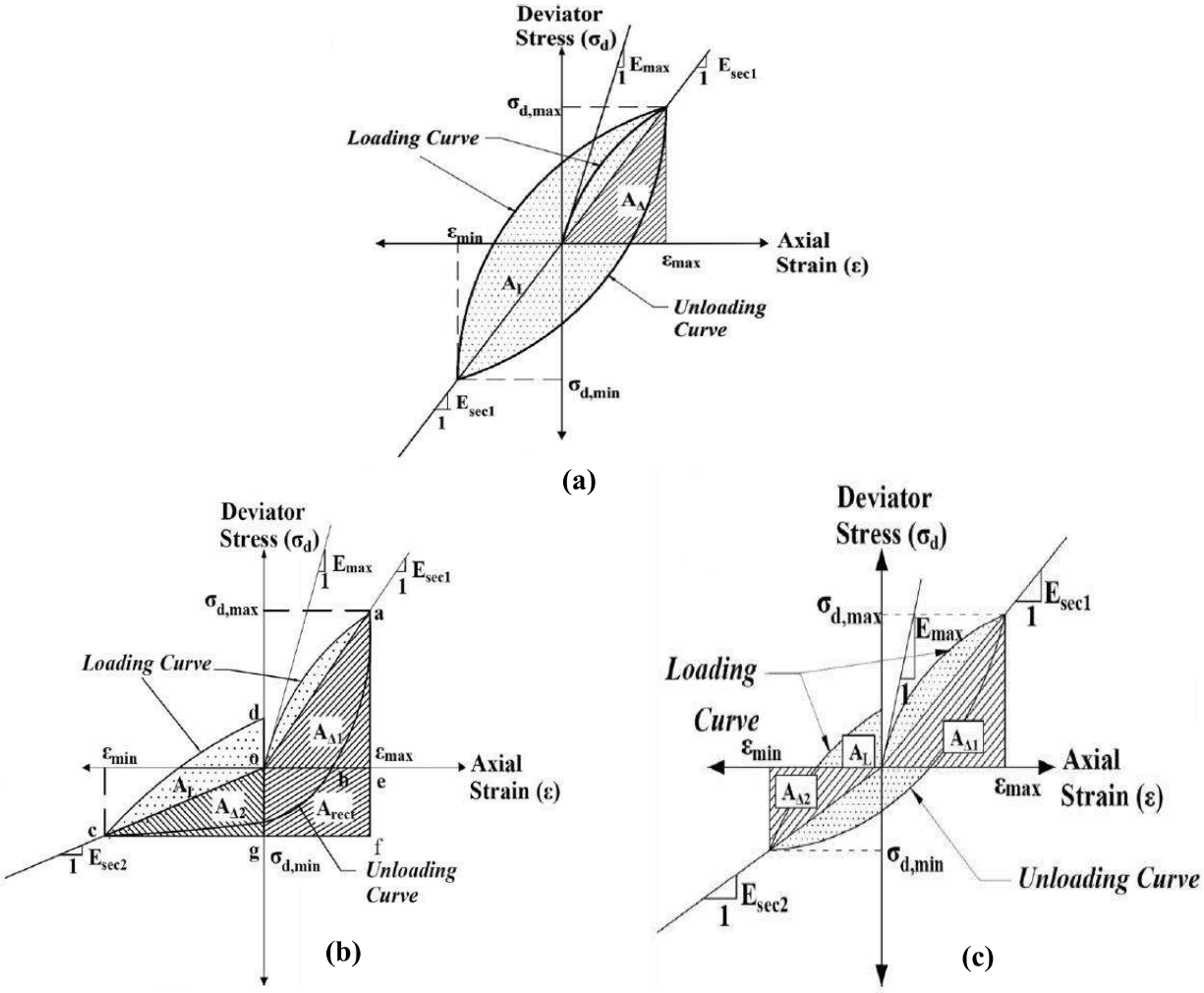

Fig. 8.1. Graphical illustration of various method such as (a) symmetrical hysteresis loop, (b) asymmetric hysteresis hysteresis loop, (c) modified ASTM method for the estimation of damping ratio. (Das and Chakrabortty 2022)

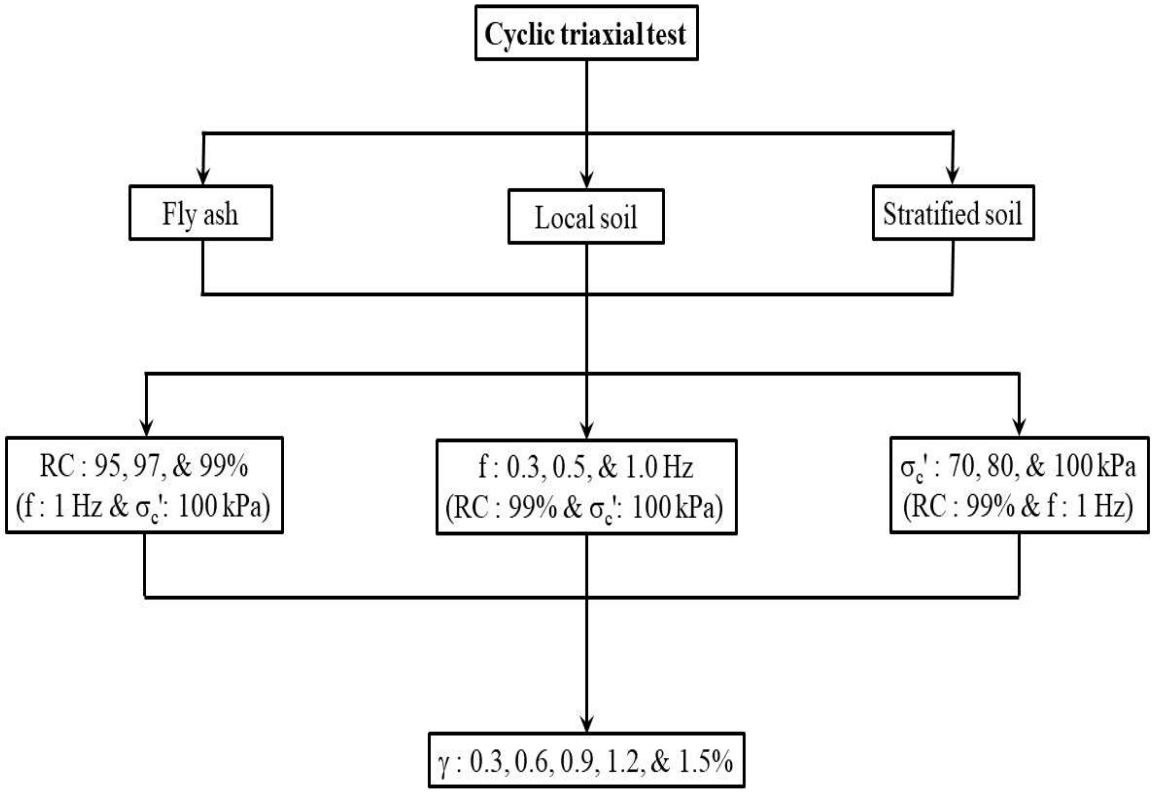

Fig. 8.2. Systematic experimental outline of testing program.

8.4 RESULTS AND DISCUSSION

Based on past earthquake studies, Tsuchida (1970) has reviewed the particle size distribution of liquefied/non-liquefied soils and suggested a grain size distribution curve for most/potentially liquefiable soil. The fly ash and local soil have also been checked for their liquefaction susceptibility through this distribution curve as shown in Fig. 8.3. About more than 50% of fly ash particles are coinciding the boundary of most liquefiable soil and 17% of the particles are falling between these two boundaries (most likely/likely to liquefy). On the other hand, local soil has almost < 5% of particles in the boundary of most liquefiable and potentially liquefiable soil. The liquefaction phenomena were frequently observed in the loose saturated sand and silty soil, therefore there exist several liquefaction studies concentrating on these types of soil (Ishihara and

Koseki 1989; Seed and Lee 1996; Dash et al. 2010; Akhila et al. 2019). The cohesionless soil has tendency of densification due to external disturbance/vibrations which is the main cause of pore pressure development that ultimately lead to the loss of shear strength and then failure. Whereas in cohesive soil, this densification is difficult due to the particle to particle attraction also known as cohesion. Hence, fine soils have been utilized by several researchers to mitigate the liquefaction potential of cohesionless soil (Guo and Prakash 2000; Marto et al. 2015; Krim et al. 2019; Ghani and Kumari 2021). The enhancement in the liquefaction resistance has also been observed by Puri (1984) and Marto et al. (2015) with the increase in fine content (clay). The present local soil contains more than 15% of clayey soil which will reduces the liquefaction tendency as compared with fly ash. Further, according to Tsuchida's chart, fly ash can be treated as partially liquefiable whereas local soil can be considered as non-liquefiable soil. Therefore, the considered materials, i.e., fly ash and local soil need to be studied thoroughly under dynamic loading conditions to understand their dynamic responses. As the damping characteristics of the material significantly affect the dynamic responses, therefore, here an attempt has been made to investigate the damping behavior of the homogeneous and stratified soil-ash specimen under dynamic loading conditions. A detailed discussion on the damping behavior of the homogeneous and stratified soil-ash samples has been reported in the subsequent sections.

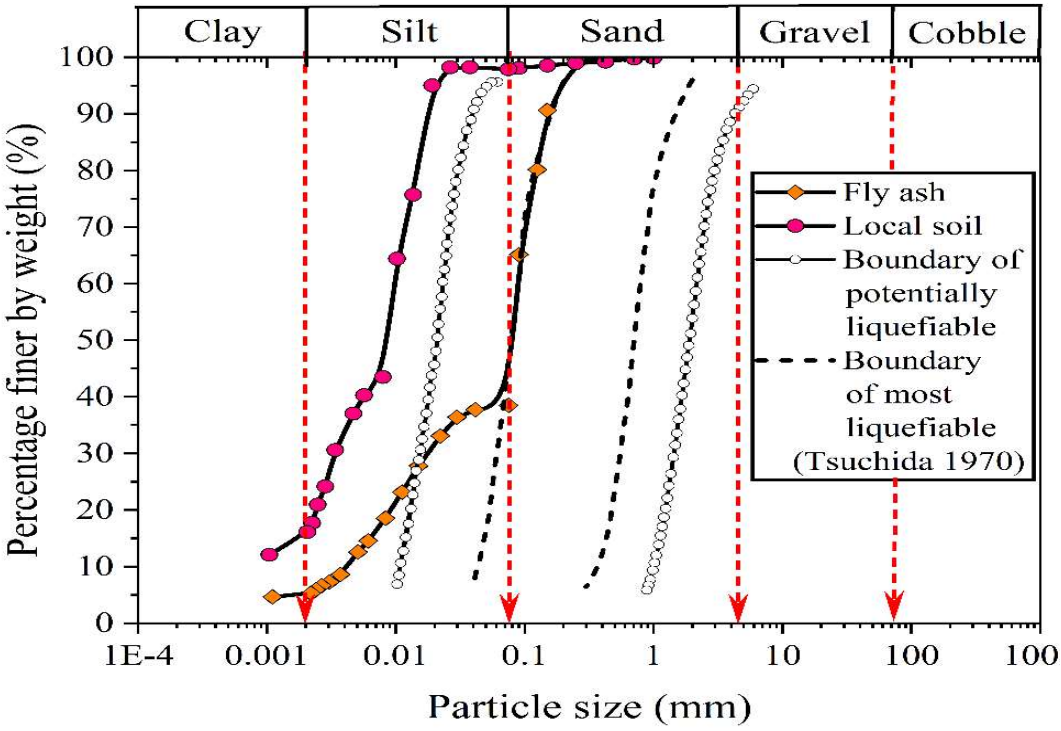

Fig. 8.3. The distribution of grains by size in the soil and ash samples used in this investigation.

8.4.1 Damping Response of Homogeneous Soil and Fly Ash Specimens

This section presents the damping (D) response of homogeneous fly ash & local soil samples under the influence of relative compaction, frequency, and confining pressure. In order to estimate the damping behavior of homogeneous soil and ash samples, the symmetric hysteresis loop approach (SHL) has been employed. The variation of damping ratio with the cyclic shear strain of both the materials considering all the variables have been shown in Fig. 8.4. From the figure, it can be seen that fly ash shows a continuous incremental trend of damping ratio till 0.6% of shear strain after that it decreases consistently with the increase in shear strain. However, the damping ratio of local soil shows an incremental trend up to 1 or 1.2% shear strain, then attains a peak and subsequently decreases. Considering the relative compaction effect, both material exhibits high damping value for lower density except at 99% density. In general, highly

compacted soil dissipates less energy under dynamic loading which ultimately results in a low damping ratio value. Similarly, for the evaluation of the frequency effect, the samples were prepared at 99% of RC and that have been subjected to an effective confining pressure of 100 kPa. From Fig. 8.4, this can be observed that both material shows a high damping value for the high frequency of loading. The confining pressure effect has been checked considering the confining pressure of 70, 80, & 100 kPa. No significant difference in damping value has been observed under different confining pressure for both of the materials (fly ash & local soil). From the above discussion, this can be inferred that the damping ratio of homogeneous soil shows a remarkable dependency on relative compaction, frequency of loading, and cyclic shear strain, and shows the least influence on confining pressure. In past studies, almost every material expressed decreasing trend of shear modulus and a corresponding increasing trend of damping ratio with an increase in shear strain. However, fly ash and local soil show a decreasing trend after peak, thus in order to determine the accurate damping behavior additional approaches (ASHL & ASTM) were incorporated here that have been explained in the subsequent sections.

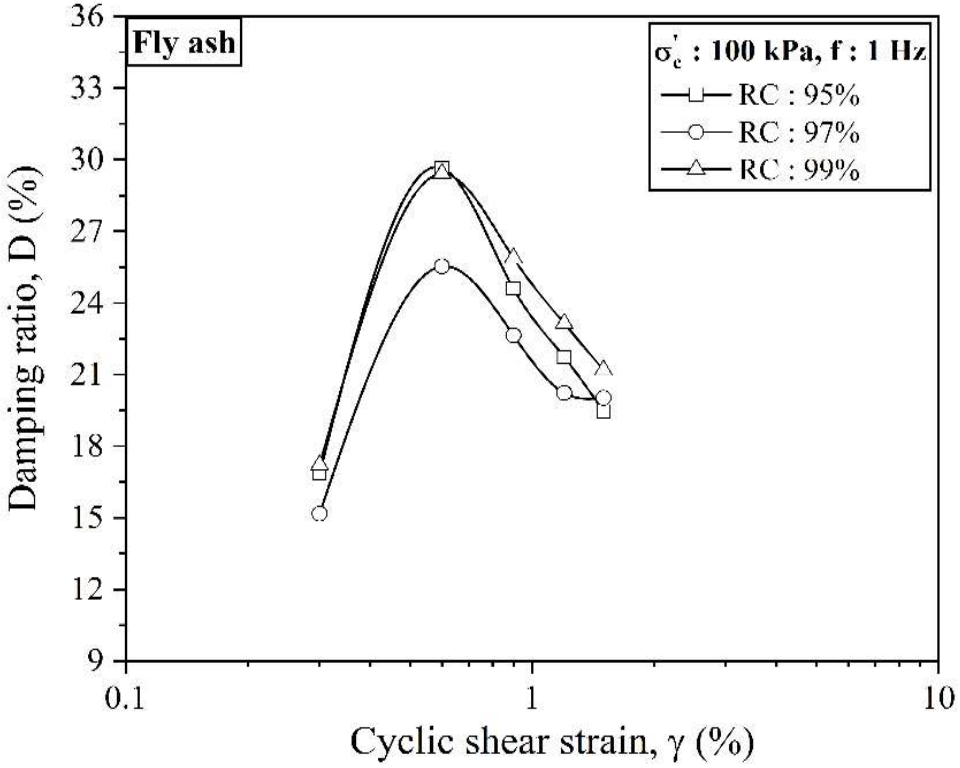
Fly ash
σ'c : 100 kPa, f : 1 Hz
RC : 95%
RC : 97%
RC : 99%
Damping ratio, D (%)
Cyclic shear strain, γ (%)
36
33
30
27
24
21
18
15
12
9
0.1
1
10

(a)

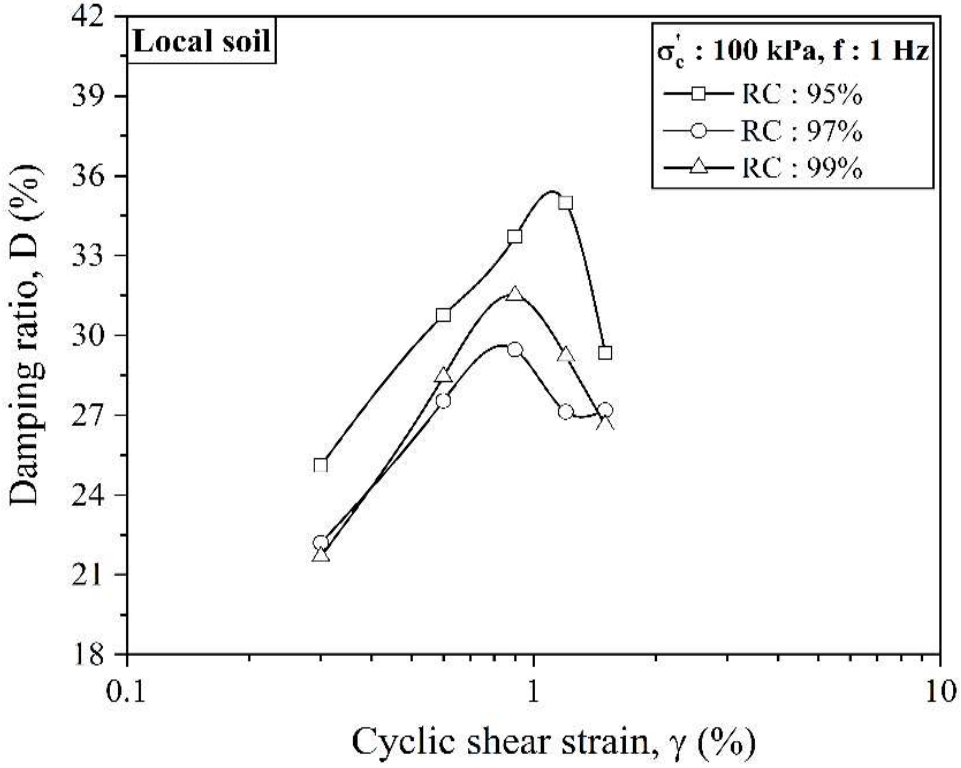
Local soil
σ'c : 100 kPa, f : 1 Hz
RC : 95%
RC : 97%
RC : 99%
Damping ratio, D (%)
Cyclic shear strain, γ (%)
42
39
36
33
30
27
24
21
18
0.1
1
10

(b)

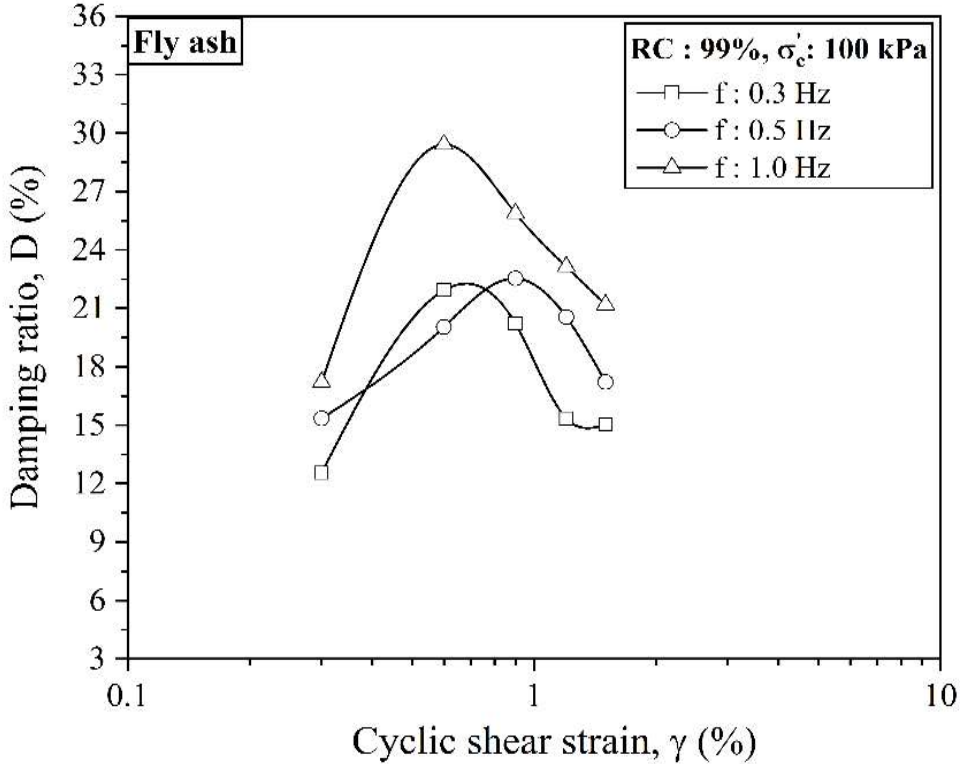
Fly ash
RC : 99%, σ'c: 100 kPa
f : 0.3 Hz
f : 0.5 Hz
f : 1.0 Hz
Damping ratio, D (%)
Cyclic shear strain, γ (%)
36
33
30
27
24
21
18
15
12
9
6
3
0.1
1
10

(c)

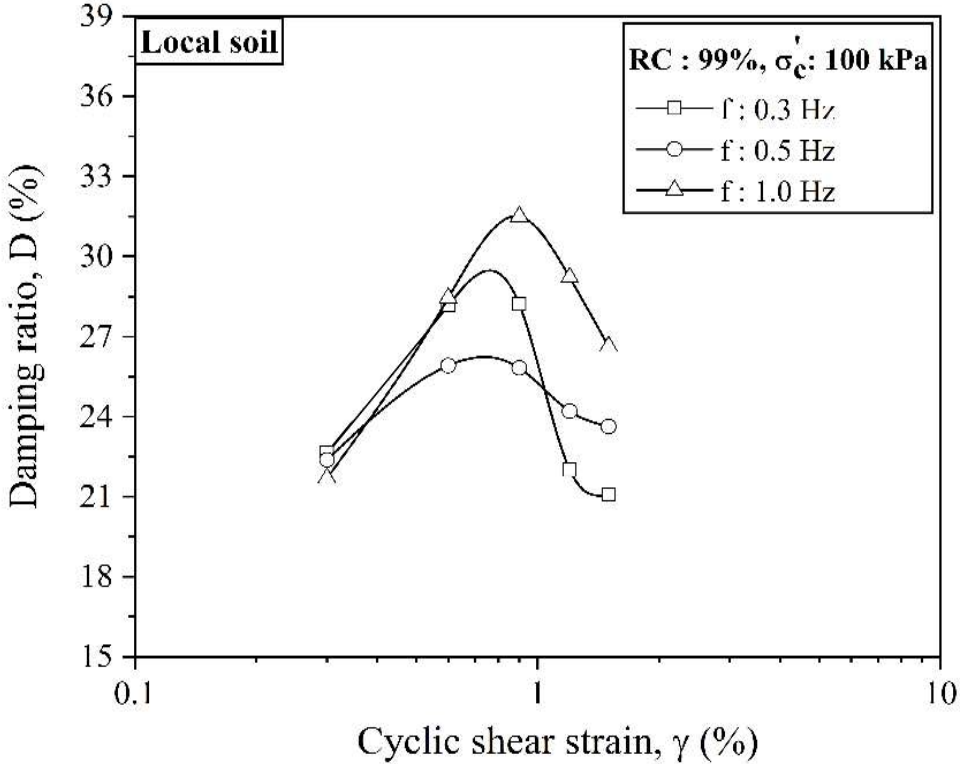
Local soil
RC : 99%, σ'c: 100 kPa
f : 0.3 Hz
f : 0.5 Hz
f : 1.0 Hz
Damping ratio, D (%)
Cyclic shear strain, γ (%)
39
36
33
30
27
24
21
18
15
0.1
1
10

(d)

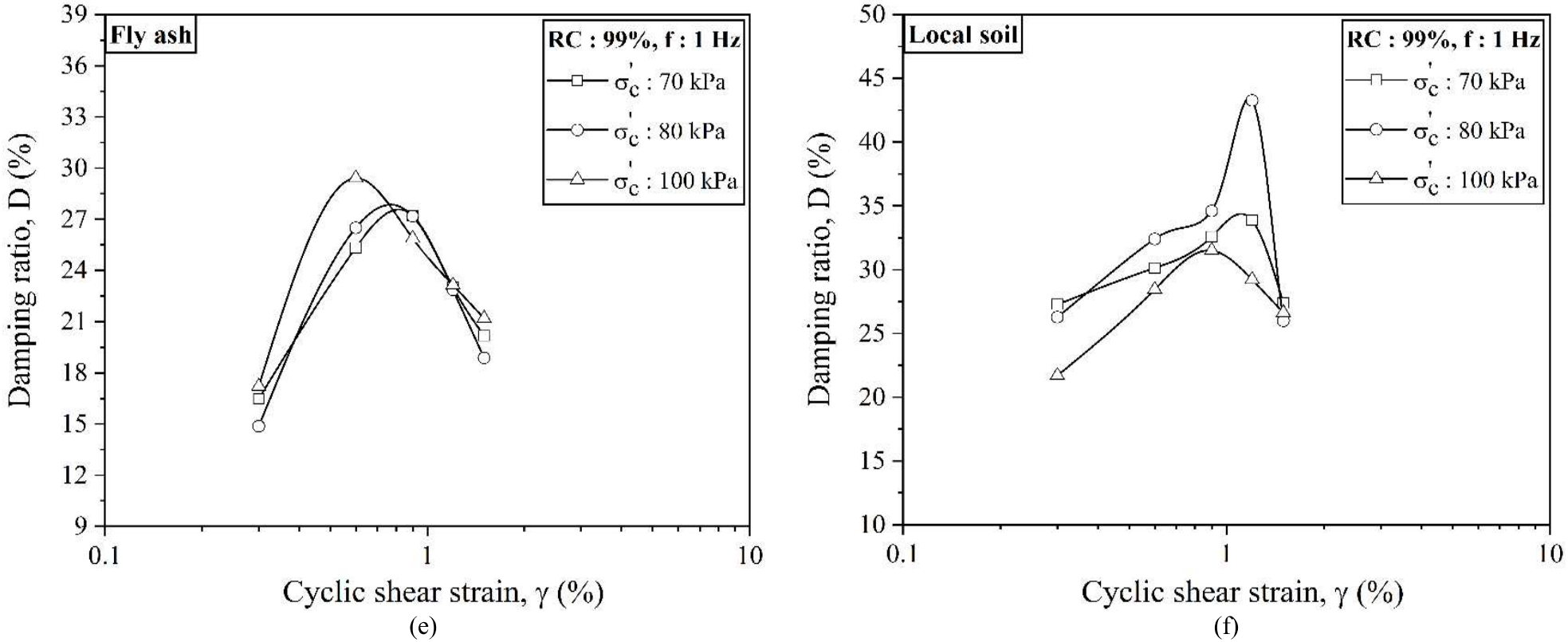

Fig. 8.4. Effect of various parameters on the damping ratio of fly ash (Ram and Mohanty 2021) and local soil for large strain.

8.4.2 Damping Response of Stratified Soil-Ash Deposit

Similar to homogeneous fly ash & local soil samples, the damping behavior of stratified soil-ash specimens has also been evaluated incorporating the influence of relative compaction, loading frequency, and confining pressure. The variation of the damping ratio with cyclic shear strain considering all the above-mentioned variables is shown in Fig. 8.5. This damping analysis was also carried out using the SHL approach. Here in the relative compaction study, the stratified soil-ash specimens show an inverse relation between the damping values and density under low shear strain. The damping nature is primarily attributed from the slippage of particles and rearrangements of particles in soil (Fahoum et al. 1996). The probability of slippage and particle rearrangements is greater in low density specimens than in high density specimens due to the availability of high voids, which eventually results in higher damping value. The difference in the damping ratio gets minimized as the shear strain increases (Fig. 8.5(a)). In this arrangement also, remarkable changes in the damping ratio value have been observed under the influence of loading frequency as shown in Fig. 8.5(b). As compared with the homogeneous soil, the stratified soil-ash arrangements show considerable variation in damping ratio with the increase in confining pressure. The trend of the damping ratio profile with cyclic shear strain is similar to homogeneous soil and it also attains its peak around 1% of shear strain.

From Fig. 8.4, this can be inferred that the peak value of damping ratio of the fly ash varies between 0.6-0.9% of shear strain, however, the local soil shows a peak in between 0.8-1.2% of shear strain. On the other hand, the stratified soil exhibits a wide range of damping ratio's peak variation, i.e., in the range of 0.6-1% of shear strain that can be seen in Fig. 8.5. The maximum damping ratio of fly ash is always lower than the maximum damping ratio of local soil. Whereas the maximum damping ratio of stratified

soil always falls in between the damping ratio of fly ash and local soil. This is due to the combined interactive behavior of fly ash and local soil composite. The percentage variation of damping ratio of fly ash varies between 100-150% and local soil varies in the range of 52-65% as compared to their minimum values. The fly ash shows a wide range of percentage variation of damping ratio, i.e., 100-150%, similarly, local soil depicts a narrow range of percentage variation of damping ratio i.e., 52-65%. From the above discussion, this can be concluded that the profile between the damping ratio versus shear strain is similar for both the homogeneous and stratified soils, but the peak of damping ratio is observed to be varied in a wide range for stratified soil. Also, the development of excess pore pressure in the stratified soil is fast as compared to the local soil due to the high permeability of fly ash.

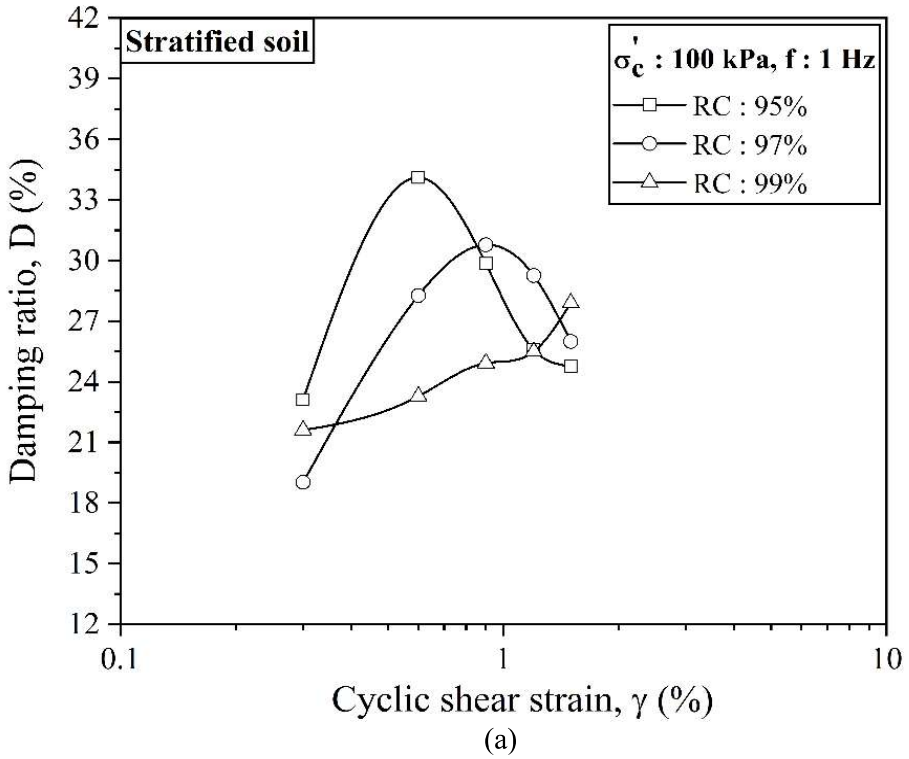

(a)

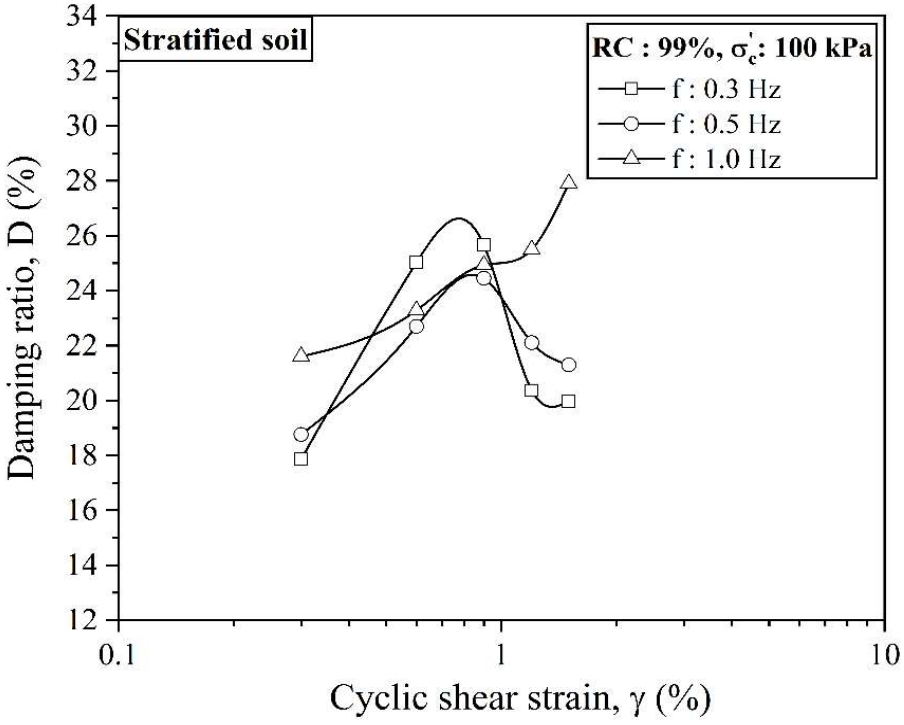

(b)

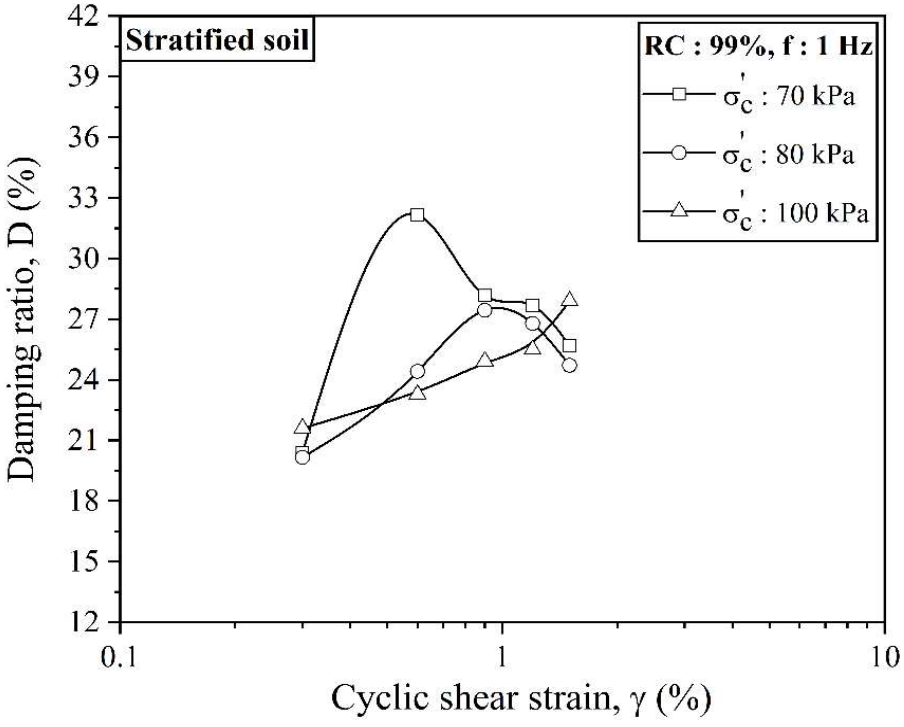

(c)

Fig. 8.5. Variation of damping ratio of stratified soil-ash samples considering all influencing parameters.

8.4.3 Identification of an Appropriate Method for the Evaluation of Damping Ratio of Homogeneous and Stratified Soil-Ash Deposit

In the present study, all the experimental studies were carried out by employing cyclic triaxial apparatus that is generally used for large strain dynamic investigation of soil. Normally a symmetric hysteresis loop (SHL) approach had been adopted for the estimation of damping ratio in past studies. The SHL approach is not reliable, especially in the case of large shear strain because under large strain the shape of the hysteresis loop becomes unsymmetrical which results in under/overestimation of the damping ratio value. Hence, in order to diminish the influence of asymmetricity in the magnitude of damping ratio, two different approaches such as ASHL and ASTM approach have been developed. The fundamental of these approaches has already been illustrated in the above-mentioned sections and their graphical & analytical equations are reported in Fig. 8.1 & Table 8.1 respectively. Here, an attempt has also been made to determine the effect of asymmetricity on the damping ratio of homogeneous and stratified soil-ash deposit under large strain conditions. The graphical representation of the damping ratio obtained from all these approaches for homogeneous and stratified soil-ash systems are depicted in Fig. 8.6 and Fig. 8.7 respectively.

In Fig. 8.6, the impact of all the variables (RC, CP, & f) on the damping ratio computed through the above-mentioned approaches for both the homogeneous materials (fly ash and local soil) are reported. The SHL approach follows an identical profile of damping ratio versus shear strain plot for all the variables as compared with the other two approaches. Whereas the ASHL approach shows an increasing trend of damping profile as observed in past literature. Among all the approaches, the ASHL approach gives a higher damping ratio value, followed by the ASTM and then the SHL approach for fly ash. The high-density sample provides a low damping value

irrespective of different approaches (Fig. 8.6(a)). A similar trend of frequency effect has been observed in the ASHL and ASTM methods as in the SHL approach (Fig. 8.6(b)). The damping ratio of fly ash samples is not much affected by the confining pressure changes as seen in Fig. 8.6(c). In the case of local soil also the ASHL approach gives higher damping values as compared with the SHL and ASTM approaches. However, the ASTM approach is not showing much difference in damping value and appears always in between the ASHL and SHL approaches. Similar kind of trends of variables in damping value has been observed in local soil as witnessed for fly ash. Hence, from the above discussion, this can be noticed that the SHL approach underestimates the damping behavior of fly ash and local soil. The ASHL approach represents the same kind of trend that had been observed in past studies for similar materials. On the other hand, the ASTM approach doesn't show significant variation in damping value and also gives more or less the same value with the increase in shear strain.

The damping characteristics of the stratified soil-ash sample have been determined in order to assess the significance of various approaches and their impact on the influencing variables. The comparison of each approach considering the effect of all the influencing variables is presented in Fig. 8.7. The stratified soil-ash also exhibits a higher damping value in the case of the ASHL approach and a lower value for the SHL approach. From Fig. 8.6 and 8.7, this can be observed that the damping profile evaluated from each method follows an increasing curve that reaches to the peak and then decreases. The maximum damping ratio was ascertained at nearly 1% of shear strain which was also discovered at the same shear strain by Matasovic and Vucetic (1993) and Kumar et al. (2018). Kiku and Yoshida (2000) and Mashiri (2014) noticed the peak damping at 0.1% and 0.23% of shear strain respectively. The reason behind

the drop in damping ratio is due to the sudden and significant rise in pore water pressure, particularly at large strain that results in frictional energy loss in the soil skeleton (Mashiri 2014). According to Matasovic and Vucetic (1993) the decrement in damping value is due to the 'S' shaping of shear stress vs shear strain curve that attributed from the dilative behavior of soil particles at large strain. After analyzing Fig. 8.6 and 8.7, numerous conclusions can be drawn, a) the SHL approach underestimates the damping property of homogeneous and stratified samples, b) the ASHL approach would be a better option for the precise estimation of the damping ratio because this method is in good agreement with the past reported results, i.e, damping estimated from SHL is always lower than the damping estimated by ASHL approach, c) the ASTM approach is not well defined as compared with the ASHL approach. The asymmetricity is predominantly attributed from the first, third, and fourth quadrant of the hysteresis loop plot between deviator stress versus axial strain. The SHL approach just takes into account the first quadrant whereas the ASTM approach takes the first and third quadrant for the estimation of damping ratio. The ASHL approach is the only approach that considered all the quadrant, that is significantly involved in the asymmetricity of the hysteresis loop which can be seen in Fig. 8.1. Hence, considering the formulation and area of loop involved, the ASHL approach can be contemplated as more realistic/practical compared with the other approaches. The average variation of the SHL and ASHL approach is around 20-60%, which is similar to the past reported studies (Das and Chakrabortty 2022; Kumar et al. 2017). Hence, especially for large strain dynamic characterization, the damping ratio must be evaluated using the method that considers asymmetricity in its calculation (i.e., the ASHL approach).

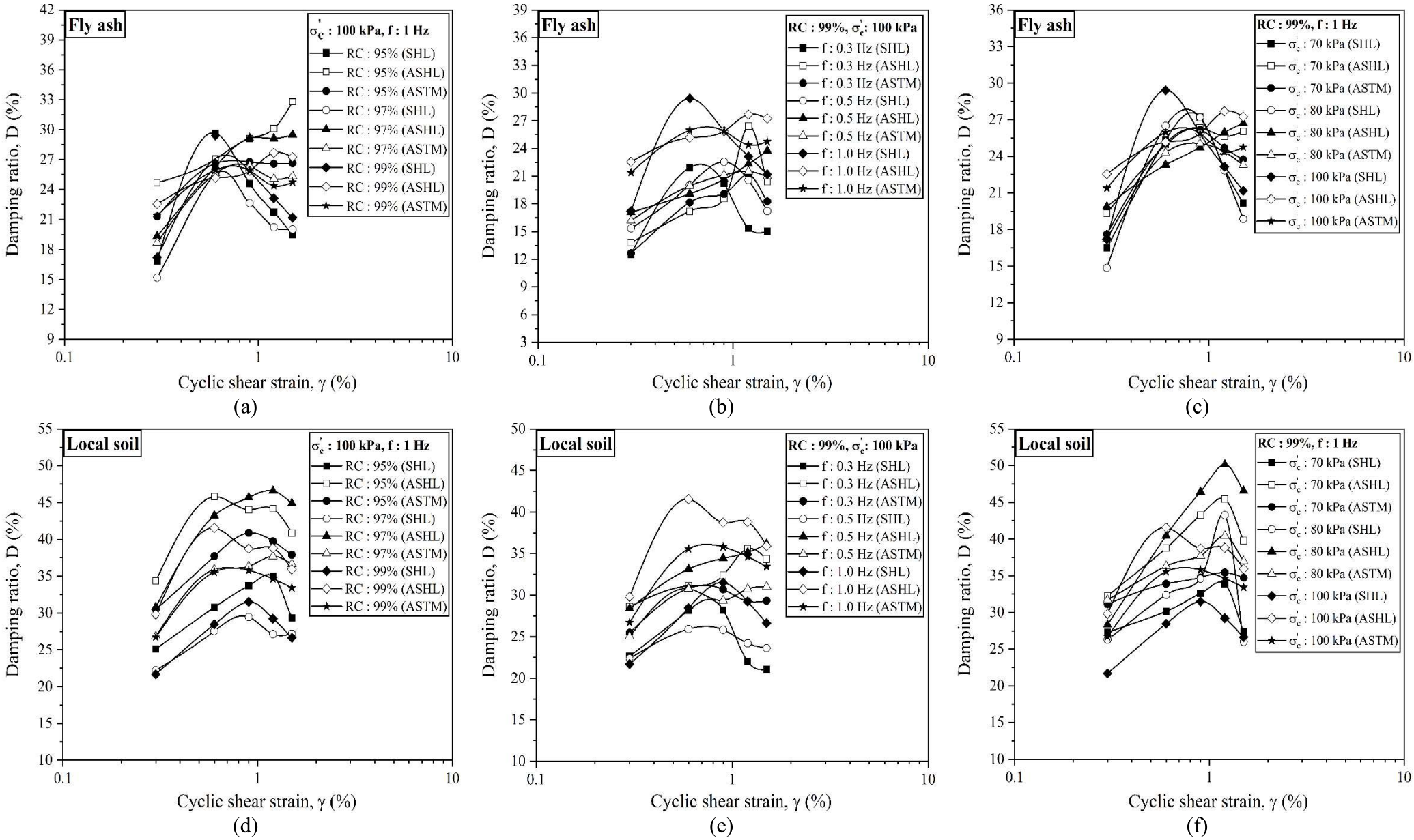

Fig. 8.6. Graphical representation of damping ratio of fly ash and local soil evaluated using SHL, ASHL, and ASTM methods.

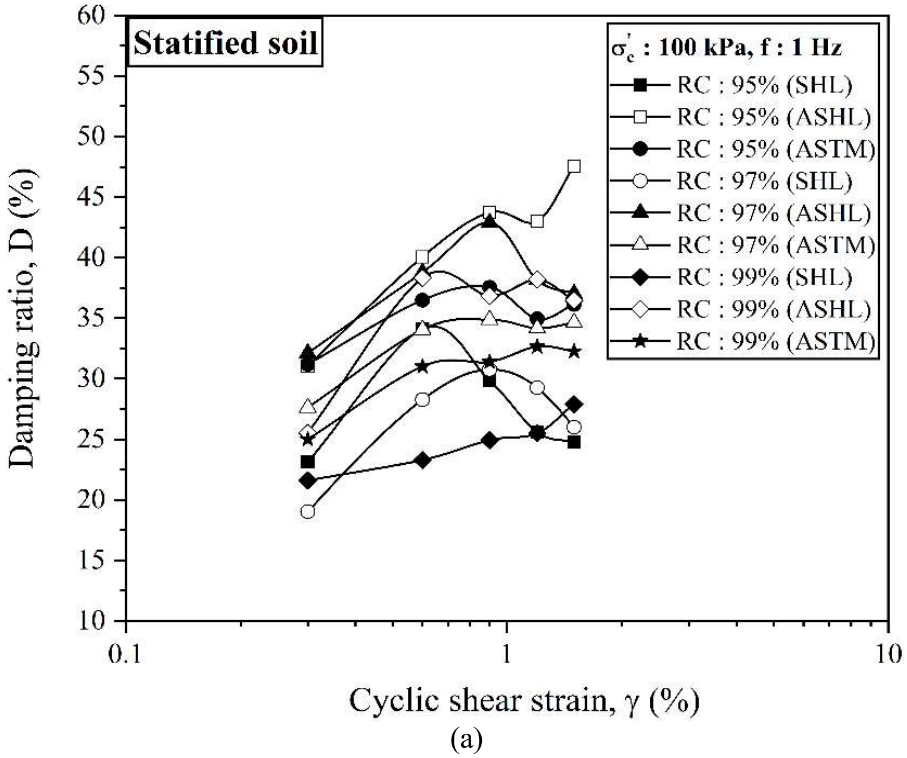
Statified soil
σ'c : 100 kPa, f : 1 Hz
RC : 95% (SHL)
RC : 95% (ASHL)
RC : 95% (ASTM)
RC : 97% (SHL)
RC : 97% (ASHL)
RC : 97% (ASTM)
RC : 99% (SHL)
RC : 99% (ASHL)
RC : 99% (ASTM)
Damping ratio, D (%)
Cyclic shear strain, γ (%)

(a)

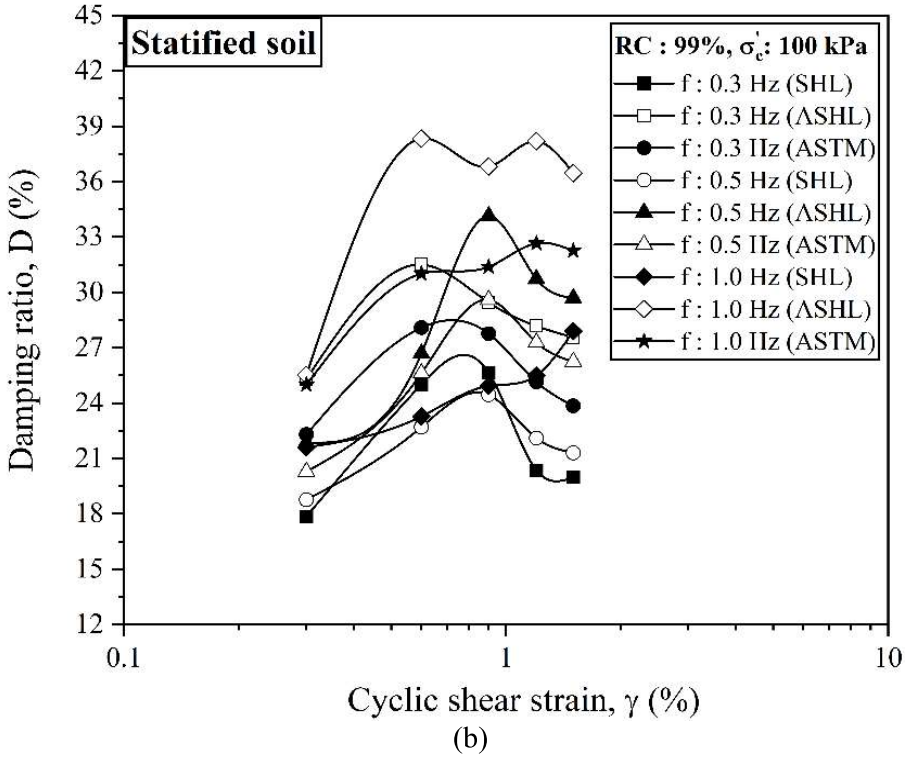
Statified soil
RC : 99%, σ'c: 100 kPa
f : 0.3 Hz (SHL)
f : 0.3 Hz (ASHL)
f : 0.3 Hz (ASTM)
f : 0.5 Hz (SHL)
f : 0.5 Hz (ASHL)
f : 0.5 Hz (ASTM)
f : 1.0 Hz (SHL)
f : 1.0 Hz (ASHL)
f : 1.0 Hz (ASTM)
Damping ratio, D (%)
Cyclic shear strain, γ (%)

(b)

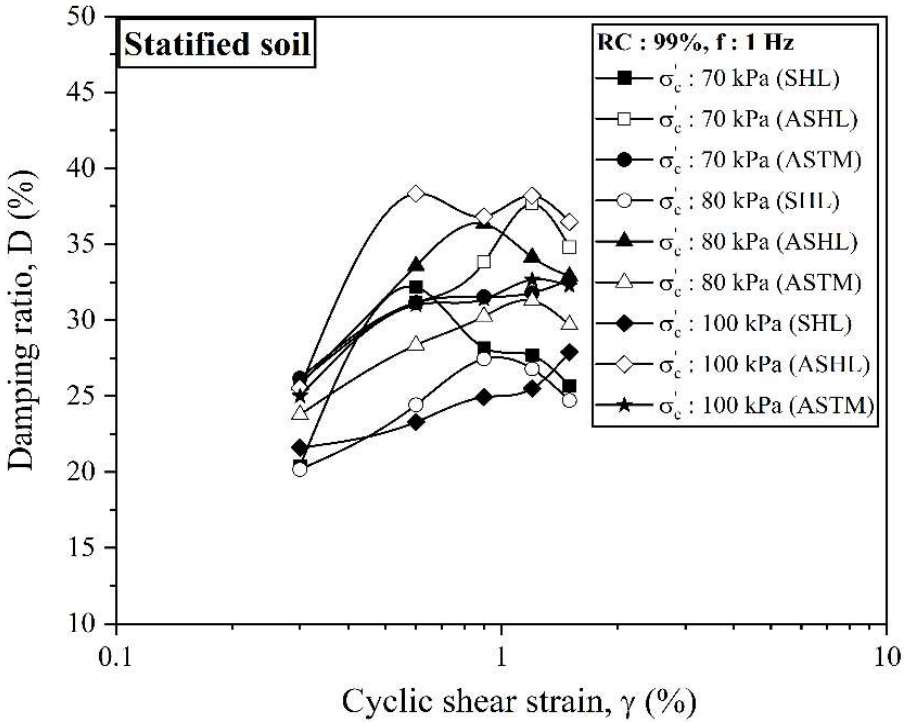

(c)

Fig. 8.7. Graphical representation of damping ratio of stratified soil-ash samples evaluated using SHL, ASHL, and ASTM methods.

8.4.4 Assessment of the Influence of Cycle Position on Damping Ratio

Conventionally, the damping ratio is estimated by implementing the 0^{th} position cycle hysteresis loop. Nevertheless, the 0^{th} position cycle may comprise flaws due to the improper contact between the top pedestal and specimen or due to the discontinuity between the start & end points of the hysteresis loop. The cycle position of the 0^{th} and 1^{st} cycle has been considered in order to identify the variation in the damping property of the homogeneous and stratified soil-ash deposits owing to cycle position. The change in the shape of the hysteresis loop under the influence of shear strain (0.6%-1.5%) for both cycles (0^{th} & 1^{st}) is shown in Fig. 8.8 & 8.9. A remarkable change in the shape of the hysteresis loop can be observed from the figures, especially for the strain 1.2% & 1.5%. The enclosed area of the hysteresis loop rises as the shear strain increases, resulting in a higher damping ratio under high strain values. Given that these tests are

strain-controlled, low resistance will emerge under low strain cyclic loading, which will result in a small size hysteresis loop. However, in the case of high strain loading, high resistance will be experienced by the sample that ultimately exhibits an increase in the length and width of the hysteresis loop. This increase in the size of the hysteresis loop can be witnessed in Fig. 8.8 & 8.9. Several researchers in the past studies have recognized a similar kind of increment in damping ratio with the increase in shear strain (Dammala et al. 2019 & 2017; Das and Chakrabortty 2022; Kokusho et al. 1982; Kumar et al. 2017). The reduction in deviator stress from the 0^{th} cycle to the 1^{st} cycle is approximately 10% for all the cases of homogeneous and stratified soil-ash deposits. This drop in deviator stress increases by approximately 13 to 23% as the shear strain reaches a large strain that can be deduced from Fig. 8.8 & 8.9. To understand the reduction phenomenon of the hysteresis loop, the area of the hysteresis loop (A_L) corresponding to each shear strain for the entire soil and ash sample has been expressed in the form of a bar chart as shown in Fig. 8.10. The same figure shows that the influence of cycle position is not remarkable for low shear strain, but for high strain, this difference in the A_L is pronounced. After analyzing the damping ratio obtained for various relative compaction, this can be inferred that the fly ash and stratified soil-ash indicate a high difference in the 0^{th} & 1^{st} cycle for the SHL approach followed by the ASTM approach and then the ASHL approach. The variation in the damping ratio between the 0^{th} & 1^{st} cycle estimated from the SHL, ASHL, and ASTM approaches are 14%, 5%, and 8% (approx.) respectively. Similarly, in stratified soil-ash samples, these variations are 8%, 2%, and 4% (approx.) for the SHL, ASHL, and ASTM approaches respectively. However, local soil shows more or less the same damping estimated from the SHL approach for both the cycles and 5% & 2% variation for the ASHL & ASTM approaches. The relative compaction and confining pressure effects show similar

variations in damping, but the change becomes more pronounced as the frequency of loading changes. Hence, from the above discussion, this can be concluded that the ASHL approach can be adapted to estimate the damping ratio using any cycle because this approach shows minimum variation than that of the others. Additionally, a critical strain must be identified because, below it, the cycle displays results that are identical, and beyond it, a substantial variation can be seen.

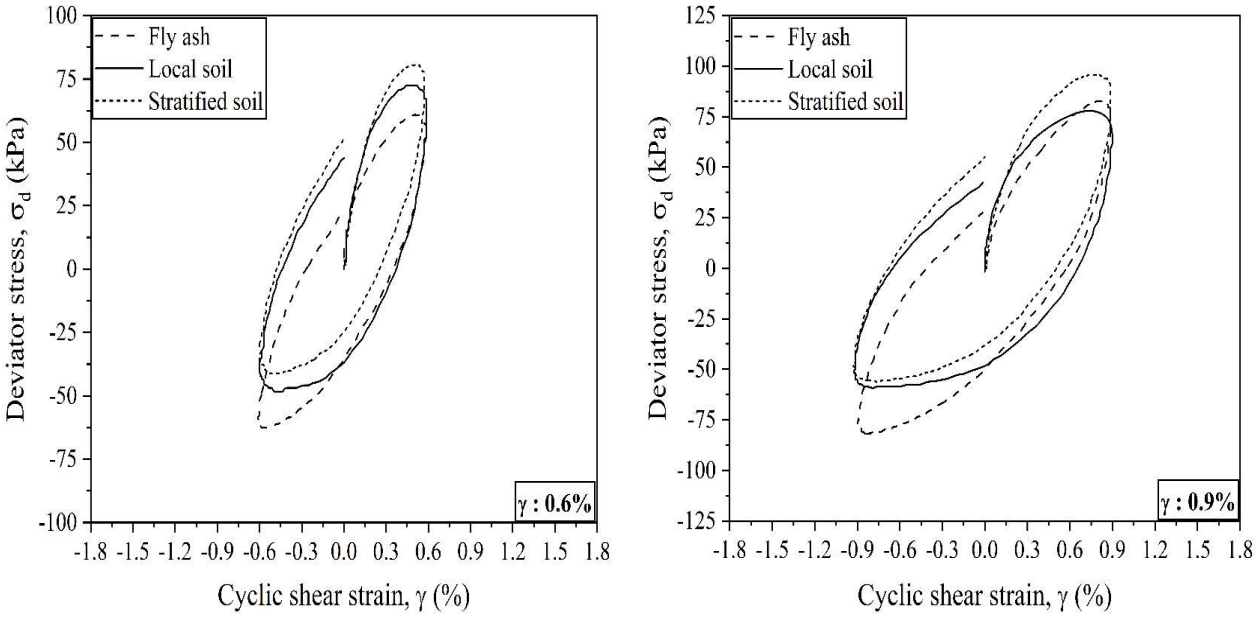

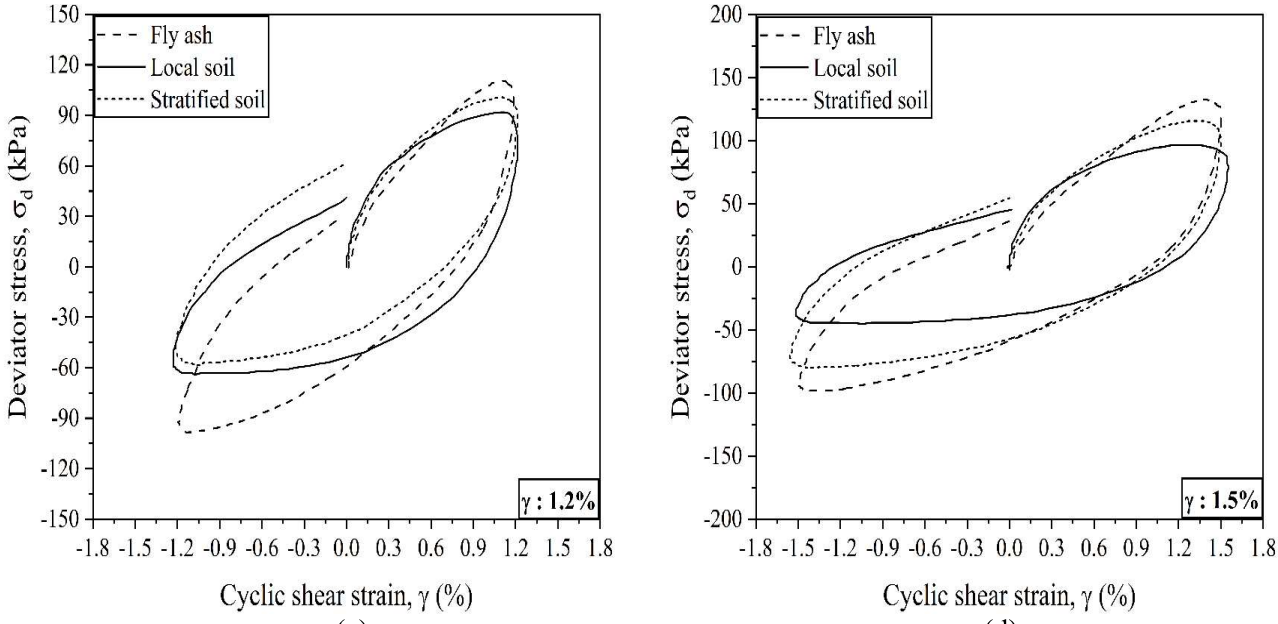

(c) (d)

Fig. 8.8. Asymmetricity of hysteresis loop at 0th cycle position under different cyclic shear strain for homogeneous and stratified soil-ash samples.

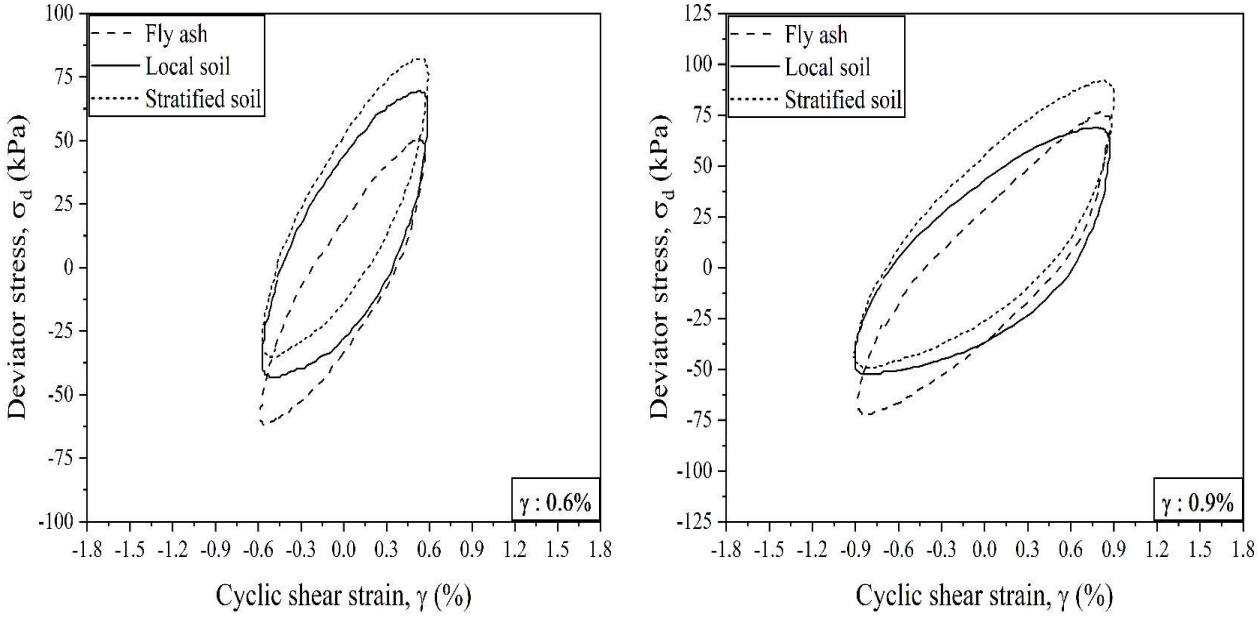

(a) (b)

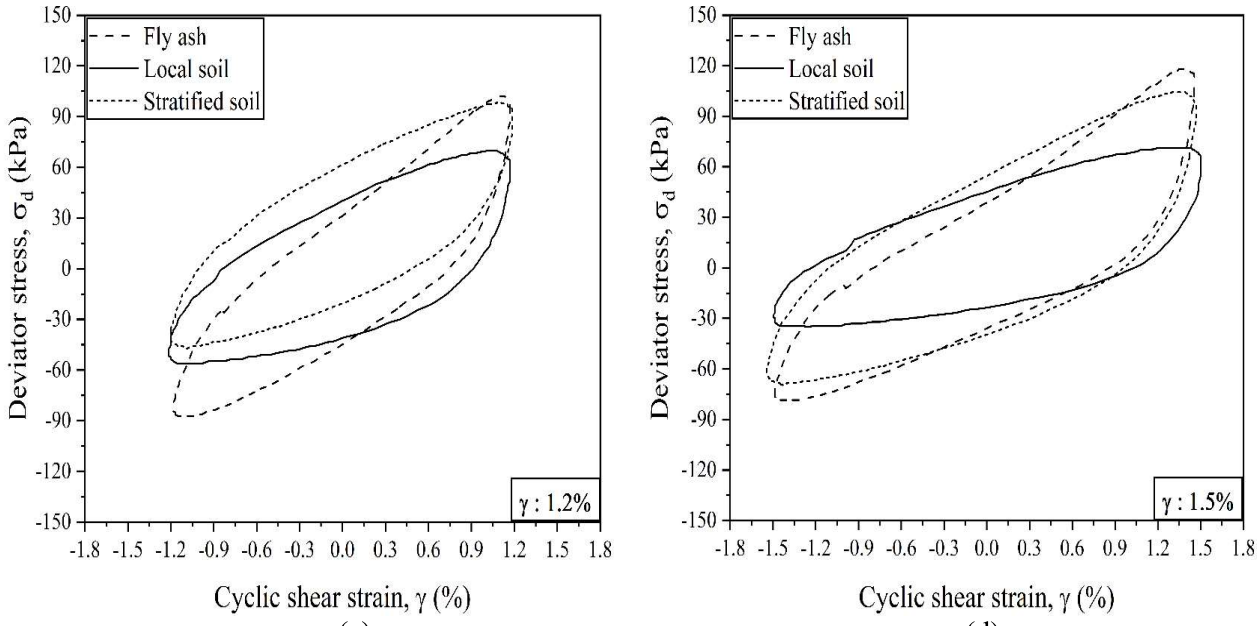

Fig. 8.9. Asymmetricity of hysteresis loop at 1st cycle position under different cyclic shear strain for homogeneous and stratified soil-ash samples.

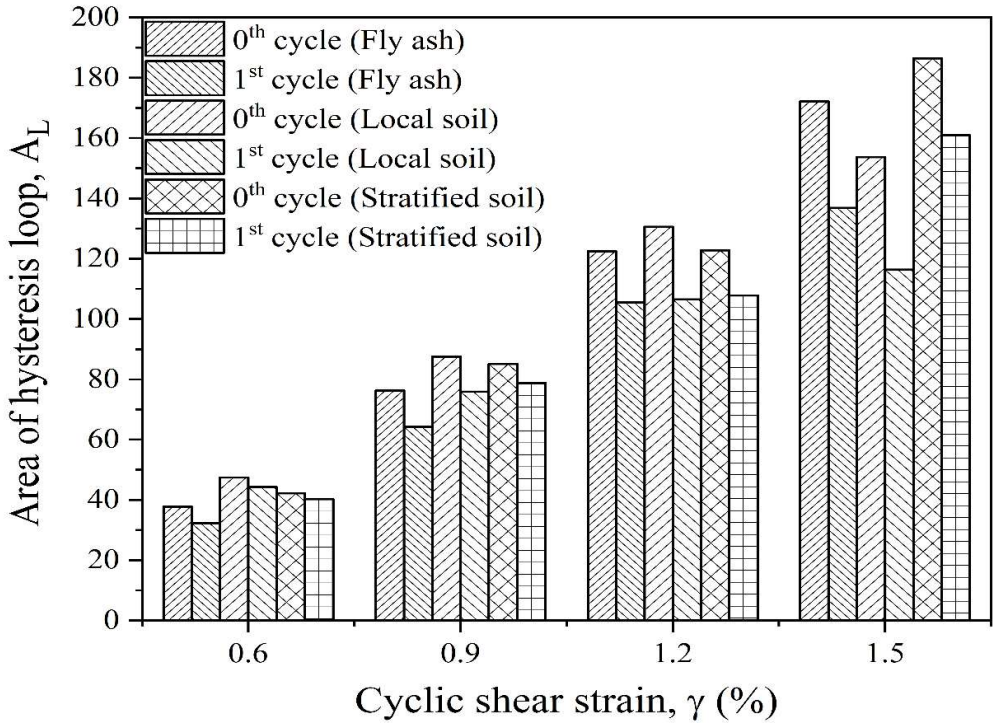

Fig. 8.10. Bar distribution of area of hysteresis loop plotted against 0th and 1st cycle position.

8.4.5 Comparison of Present Study Results with Past Literature

The outcomes of the damping ratio of the present study under the influence of relative compaction (RC: 95, 97, 99%), confining pressure (CP: 70, 80, 100 kPa), and loading frequency (f: 0.3, 0.5, 1.0 Hz) are compared with the past reported results of soils (Fig. 8.11 and 8.12). Here, the damping ratio estimated from the ASHL (0^{th} cycle) approach is used for comparison purposes. Because the ASHL approach is a novel approach that incorporates the unsymmetrical shape of the hysteresis loop for the precise estimation of the damping ratio. The soil types considered in the comparison are river sand, Toyoura sand, clay, sandy silt, gravelly rockfill, etc. (Amir-Faryar et al. 2017; Araei et al. 2012; Chattaraj and Sengupta 2016; Chehat et al. 2019; Chiaradonna et al. 2015; Das and Chakrabortty 2022; Govindaraju 2005; HanumanthaRao and Ramana 2008; Kiku and Yoshida 2000; Kokusho 1980; Kumar et al. 2014; Li et al. 2020; Matasović and Vucetic 1993; Mog and Anbazhagan 2022; Pagliaroli et al. 2018; Ravishankar et al. 2005; Vucetic and Dobry 1991). Additionally, the soil of various origins depicted in Fig. 8.13 is used to analyze the range of damping ratio of the current materials for a realistic interpretation. Kumar et al. (2017) investigated the damping behavior of Brahmaputra sand for large strain conditions using cyclic triaxial test and found that under large strain the damping ratio increases till critical strain reaches its peak and then decreases. Since limited researchers had explored the dynamic behavior beyond 1%, thus it is recommended to perform dynamic testing further on this strain. So that critical strain can be identified for better seismic analysis of a particular soil. Specimen prepared at high density shows lower damping value compared to the samples prepared at low density and from Fig. 8.11(a) this can be confirmed for the present materials. But a contradictory result has been obtained by Mog and Anbazhagan (2022). Similarly, a specimen subjected to high confinement may impart high stiffness that in turn

increases the shear modulus and decreases the damping ratio. The present results are in good agreement with the past results illustrated in Fig. 8.11(b). The high damping ratio obtained from the ASHL approach for the present materials is compared with the past results in Fig. 8.11 and 8.12. The SHL approach underestimates the damping value and the same can be seen in Fig. 8.6 and 8.7 and also similar trend has been observed by several researchers (Das and Chakrabortty 2021; Kumar et al. 2017). The specimen subjected to a high loading frequency dissipates high energy which contributes to high damping values. From Fig. 8.12, this can be observed that irrespective of the material type high frequency exhibits a high damping value. The damping value of the present fly ash is in good agreement with the Sabarmati river sand and Xiamen standard sand (Li et al. 2020; Ravishankar et al. 2005). Mog and Anbazhagan (2022) performed a resonant column test on the sand and clayey samples and reveals that the clayey silt soils experience high damping value than that of the sandy soil. At large strain, each soil is showing a damping value between 10% to 30% (Fig. 8.13), and the damping value estimated using the SHL approach is also coming within this range (Fig. 8.6 and 8.7). The trend of damping ratio with shear strain shows good agreement with the past reported results. The damping assessment of any soil must be done for a wide strain (small-medium-large) range so that its complete profile can be established. Since this study was done only for large strain conditions that exhibit the limitation of the present study. A wide strain range can be considered as the future scope of this research.

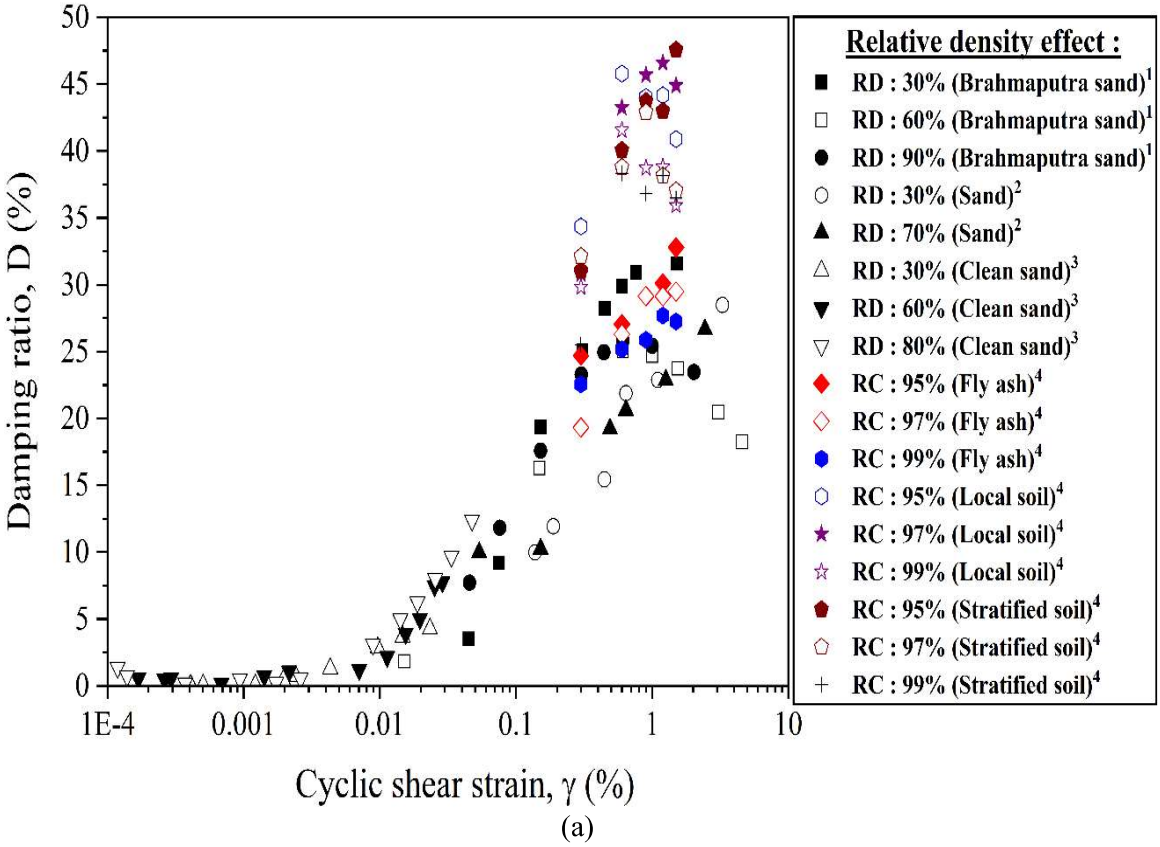
Damping ratio, D (%)
Cyclic shear strain, γ (%)
50
45
40
35
30
25
20
15
10
5
0
1E-4
0.001
0.01
0.1
1
10
Relative density effect :
RD : 30% (Brahmaputra sand)[1]
RD : 60% (Brahmaputra sand)[1]
RD : 90% (Brahmaputra sand)[1]
RD : 30% (Sand)[2]
RD : 70% (Sand)[2]
RD : 30% (Clean sand)[3]
RD : 60% (Clean sand)[3]
RD : 80% (Clean sand)[3]
RC : 95% (Fly ash)[4]
RC : 97% (Fly ash)[4]
RC : 99% (Fly ash)[4]
RC : 95% (Local soil)[4]
RC : 97% (Local soil)[4]
RC : 99% (Local soil)[4]
RC : 95% (Stratified soil)[4]
RC : 97% (Stratified soil)[4]
RC : 99% (Stratified soil)[4]

(a)

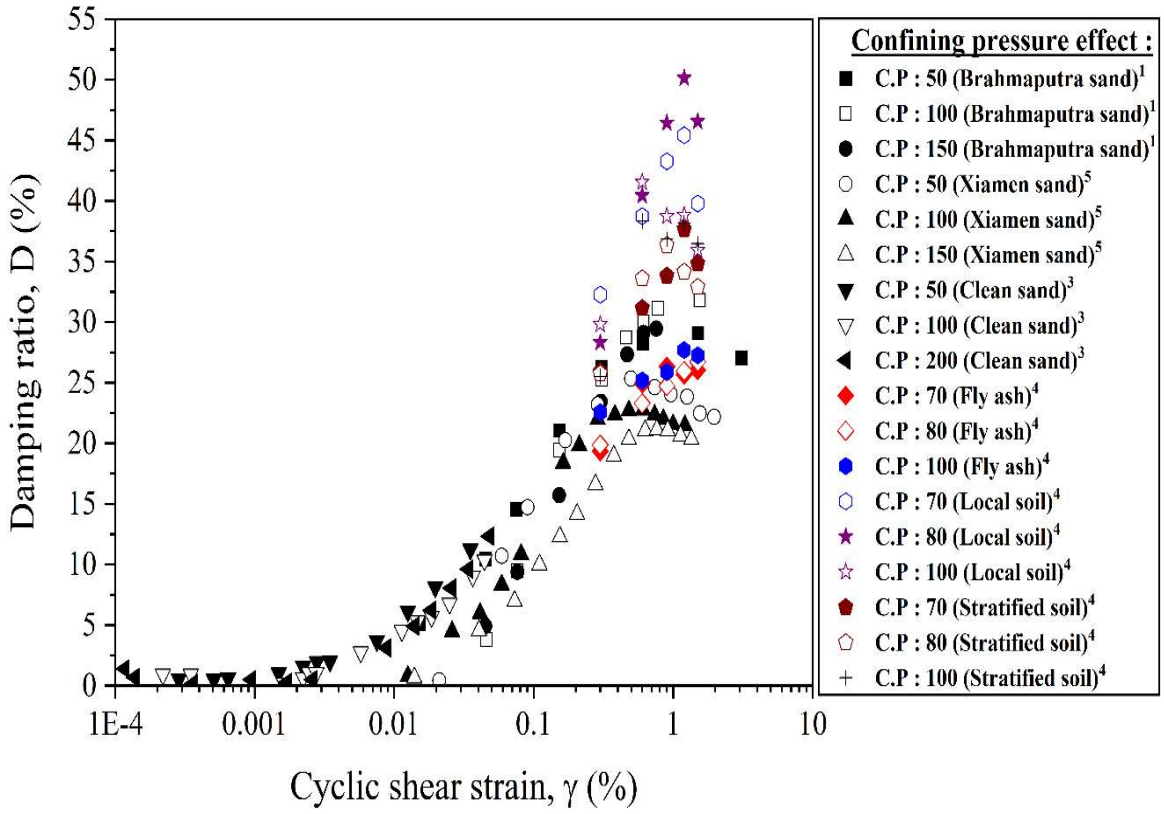

(b)

Fig. 8.11. Assessment of damping characteristics of present study results with different types of soil considering the effect of relative compaction and confining pressure. ([1] : Kumar et al. (2014); [2] : RaviShankar et al. (2012); [3] : Mog and Anbazhagan (2022); [4] : Present study; [5] : Li et al. (2020)

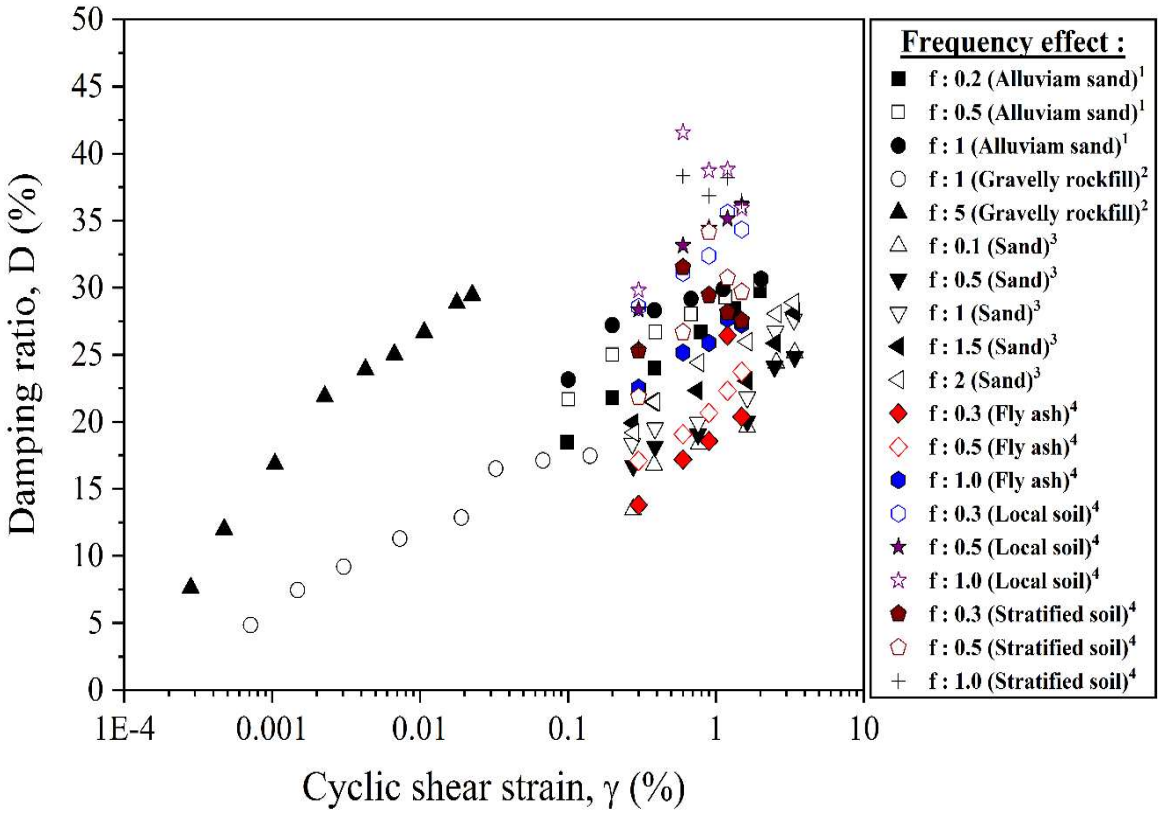

Fig. 8.12. Assessment of damping ratio of present study results with different types of soil under the influence of frequency of loading. ([1] : Das and Chakraborty (2021); [2] : Aghaeiraei et al. (2012); [3] : RaviShankar et al. (2012); [4] : Present study)

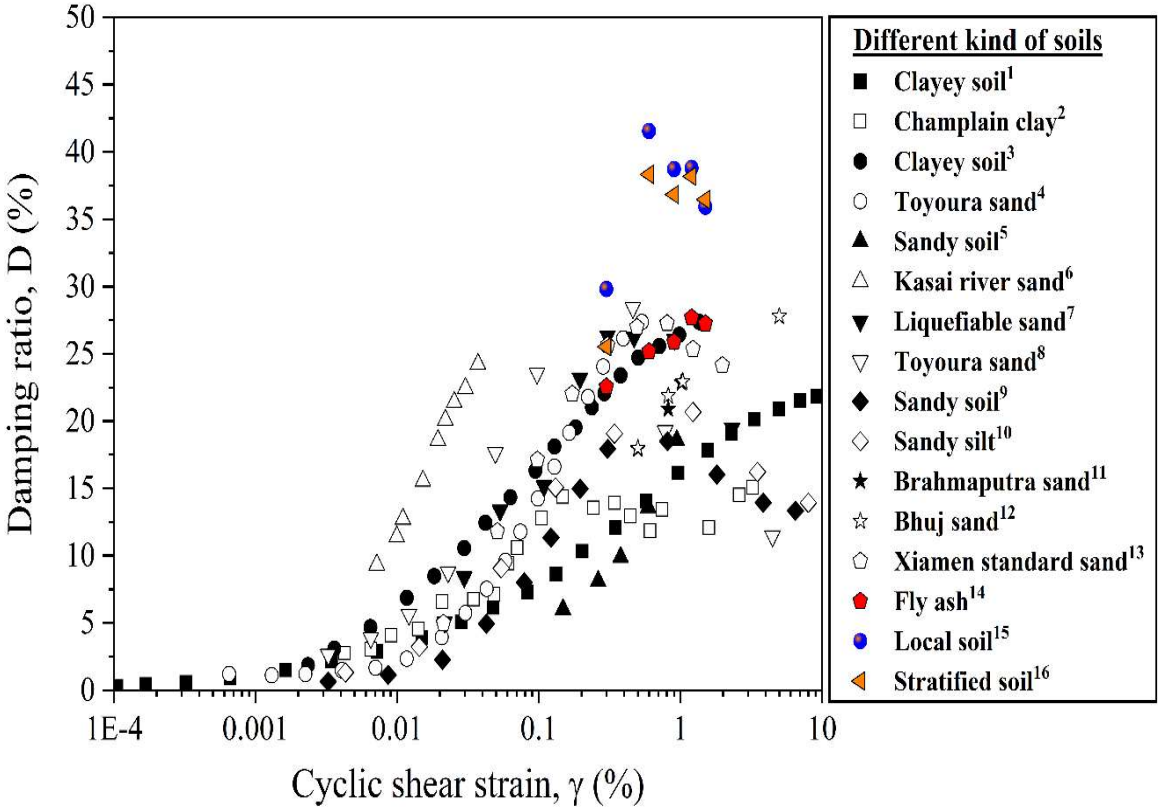

Fig. 8.13. Comparison of damping ratio of present study results with different types of soil. ([1] : Amir-Faryar et al. (2017); [2] : Chehat et al. (2018); [3] : Vucetic and Dobry (1991); [4] : Kokusho (1980); [5] : Hanumantharao and Ramana (2008); [6] : Chattaraj and Sengupta (2016); [7] : Matasovic and Vucetic (1994); [8] : Kiku and Yoshida (2000); [9] : Chiaradonna et al. (2015); [10] : Pagliaroli et al. (2018); [11] : Kumar et al. 2014; [12] : Govindaraju et al. 2012; [13] : Li et al. 2020; [14,15,16] : Present study).

8.5 SUMMARY

The damping behavior of fly ash, local soil, and their stratified system has been evaluated under large strain conditions using the cyclic triaxial test. The specimens were subjected to a large shear strain range of 0.3 to 1.5% under the loading frequency of 0.3 to 1 Hz. In addition, the density of the compacted specimens was maintained between 95 to 99% of maximum dry density and tested under a medium range of confining pressure (70 to 100 kPa). The present experimental study was carried out by applying high strain amplitude loading that resulted in an unsymmetrical response of deviator stress vs. axial strain. In order to analyze the unsymmetrical phenomena in the damping behavior of soil, the damping ratio was estimated by incorporating three different approaches such as SHL, ASHL, and ASTM approaches.

The study focused on estimating the damping ratio of fly ash, local soil, and stratified soil-ash samples using different approaches and under various conditions. The following key findings emerge from the experimental outcomes: The damping ratio of the fly ash, estimated using both the symmetrical (SHL) and asymmetrical (ASHL) approaches, exhibits a similar trend, with the maximum damping ratio occurring at around 1% of shear strain. The density and confinement conditions of the specimens affect the damping ratio, with high-density and highly confined specimens showing lower damping ratios. Conversely, specimens tested under high-frequency conditions exhibit higher damping behavior. The SHL approach is suitable for the low-strain conditions, as it tends to underestimate the damping ratio of soils under large-strain conditions. Among the different approaches, the ASHL approach yields the highest damping ratio, followed by the ASTM approach, and then the SHL approach, for fly ash, local soil, and stratified soil-ash samples. The influence of cycle position on the damping ratio is not significant for the low shear strain, but for high strain levels, the

difference in the A_L is more pronounced. The ASHL approach is recommended for estimating the damping ratio using data from any cycle position, as it exhibits minimal variation compared to the other approaches. The maximum damping ratio of the stratified soil-ash deposit consistently falls between the damping ratios of the local soil and fly ash. This is attributed to the combined interaction between the fly ash and local soil components. The peak damping ratio of the fly ash typically occurs between 0.6% and 0.9% of shear strain, while the local soil shows a peak between 0.8% and 1.2% of shear strain. In contrast, the stratified soil exhibits a wider range of peak damping ratio variation, spanning 0.6% to 1% of shear strain. Overall, the study provides insight into the damping behavior of the fly ash, local soil, and stratified soil-ash samples under different approaches, conditions, and strain levels. These findings can guide the estimation of damping ratios and enhance the understanding of the dynamic response of these materials in various engineering applications.